

## SOLUTION FOR THE THERMAL ENTRY REGION IN LAMINAR FLOW OF BINGHAM PLASTICS WITHIN ANNULAR DUCTS VIA INTEGRAL TRANSFORMATION

**Udilma da Conceição Serrão Nascimento**

Chemical Engineering Department-CT/Universidade Federal do Pará-UFPA

**Emanuel Negrão Macêdo**

Mechanical Engineering Department-CT/Universidade Federal do Pará-UFPA

**João Nazareno Nonato Quaresma**

Chemical Engineering Department-CT/Universidade Federal do Pará-UFPA

Campus Universitário do Guamá, Rua Augusto Corrêa, 01

66075-900 - Belém, PA, Brasil - E-mail:quaresma@ufpa.br

**Abstract.** *The thermal entry region in laminar flow of Bingham plastics within concentric annular ducts is solved analytically through the classical integral transform technique. Boundary conditions of first kind are prescribed either at inner or outer wall duct in order to verify the effects on the temperature field in the fluid. Nusselt numbers are calculated along both the thermal entry and fully-developed regions with high accuracy for different yield numbers and aspect ratios which are systematically tabulated and graphically presented.*

**Keywords:** *Bingham plastics; Annular ducts; Integral transform.*

### 1. INTRODUCTION

Viscoplastic materials are those that present a minimum shear stress termed as yield stress, which must be exceeded in order to start the flow. Rheological models included into this category are those that follow the Herschel-Bulkley model or a Bingham plastic model (Bird *et al.*, 1987), which is one of the simplest equation that describes the behavior of viscoplastic materials.

There are numerous industrial applications involving fluids behaving in this manner, mainly in chemical, pharmaceutical, food, petroleum and petrochemical industries where we can find the processing of toothpaste, molten plastics, aqueous foams, slurries and paper pulp. Bird *et al.* (1982) have done an extensive compilation of materials presenting a yield stress.

An important industrial application concerning to flow of a Bingham plastic is that where during a drilling operation in the petroleum industry certain muds are pumped through the annular space between the drill and the well, in order to provide a good operation and the well cementing. These muds generally are described for a Herschel-Bulkley model, but under certain circumstances the Bingham plastic model can be employed to characterize their

behavior. The physical properties of these fluids are very sensitive to the temperature, and consequently this affects the velocity profile and the temperature field itself, which are important roles for the complete control of the drilling operation.

Few works dealing with the heat and fluid flow of Bingham plastics within concentric annular ducts are encountered in the literature despite their important industrial applications, as that pointed out above. Among these works are included those by Laird (1957), Fredrickson and Bird (1958) and Anshus (1974), in these works the authors have determined the complete characteristics of the flow. On the other hand, heat transfer problems in which viscoplastic materials such as Bingham fluids or Herschel-Bulkley fluids are involved, mostly concern to circular duct and parallel-plates geometry as those by Forrest and Wilkinson (1973), Blackwell (1985), Nouar *et al.* (1994, 1995), Mendes and Naccache (1995), Vradis *et al.* (1993), Min *et al.* (1997) and Vradis and Hammad (1995).

Thus, in this context, the present work aims at advancing the ideas of the classical and generalized integral transform techniques and the so-called sign-count approach in order to determine the characteristics of the heat and fluid flow of Bingham plastics within annular passages, by calculating the product between the friction factor and Reynolds number, as well as, Nusselt numbers along both, the thermal entry and fully-developed regions, with high accuracy. Comparisons with previous works in the literature are performed, for typical situations, in order to validate the numerical code developed here.

## 2. ANALYSIS

The rheological behavior of the non-newtonian fluid described here is given by the Bingham plastic model in the following form:

$$\tau_{rz} = \pm \tau_0 - \mu_0 \frac{du}{dr} ; \quad \text{if } |\tau_{rz}| \geq \tau_0 \quad (1.a)$$

$$\frac{du}{dr} = 0 ; \quad \text{if } |\tau_{rz}| < \tau_0 \quad (1.b)$$

where,  $\tau_{rz}$  is the shear stress,  $\tau_0$  is the yield stress and  $\mu_0$  is the plastic viscosity of the fluid. Here the + sign is used when the transport of momentum is done in the + r-direction and the - sign is used when momentum is being transported in the - r-direction.

For the fully-developed region of a concentric annular duct, the momentum equation in the axial coordinate z, is simplified to yield:

$$\frac{1}{r} \frac{d}{dr} (r \tau_{rz}) = \left( - \frac{dp}{dz} \right), \quad \text{in } r_{iw} < r < r_{ow} , \quad z > 0 \quad (2.a)$$

subjected to the following boundary conditions

$$u = 0 \quad \text{at } r = r_{iw} \quad \text{and} \quad u = 0 \quad \text{at } r = r_{ow} \quad (2.b, c)$$

Then, introducing Eqs. (1) in Eq. (2.a), and after the integrations are performed, the fully-developed velocity profile in three ranges for Bingham plastic fluids is given by:

$$u^-(r) = \frac{\tau_0 r_{iw}}{\mu_0} \left( 1 - \frac{r}{r_{iw}} \right) + \frac{\left( - \frac{dp}{dz} \right) r_{iw}^2}{4\mu_0} \left( 1 - \frac{r^2}{r_{iw}^2} \right) + \frac{\left( - \frac{dp}{dz} \right) a^* b^*}{2\mu_0} \ln \left( \frac{r}{r_{iw}} \right), \quad \text{for } r_{iw} \leq r \leq a^* \quad (3.a)$$

$$u^0(r) = \begin{cases} -\frac{\tau_0}{\mu_0}(a^* - r_{iw}) - \frac{\left(-\frac{dp}{dz}\right)}{4\mu_0}(a^{*2} - r_{iw}^2) + \frac{\left(-\frac{dp}{dz}\right)a^*b^*}{2\mu_0} \ln\left(\frac{a^*}{r_{iw}}\right) \\ -\frac{\tau_0}{\mu_0}(r_{ow} - b^*) + \frac{\left(-\frac{dp}{dz}\right)}{4\mu_0}(r_{ow}^2 - b^{*2}) + \frac{\left(-\frac{dp}{dz}\right)a^*b^*}{2\mu_0} \ln\left(\frac{b^*}{r_{ow}}\right) \end{cases}, \text{ for } a^* \leq r \leq b^* \text{ (3.b,c)}$$

$$u^+(r) = \frac{\tau_0 r_{ow}}{\mu_0} \left( \frac{r}{r_{ow}} - 1 \right) + \frac{\left(-\frac{dp}{dz}\right) r_{ow}^2}{4\mu_0} \left( 1 - \frac{r^2}{r_{ow}^2} \right) + \frac{\left(-\frac{dp}{dz}\right) a^* b^*}{2\mu_0} \ln\left(\frac{r}{r_{ow}}\right), \text{ for } b^* \leq r \leq r_{ow} \text{ (3.d)}$$

where  $a^*$  and  $b^*$  are the bounds on the plug-flow region,  $c^*$  is the value of the radial coordinate for which the shear stress is zero. The velocity profile on the plug-flow region  $u^0(r)$  is given by Eq. (3.b) or (3.c), these equations are obtained by making  $r = a^*$  in Eq. (3.a) and  $r = b^*$  in Eq. (3.d), respectively, and they furnish the same values for the velocity profile  $u^0(r)$ .

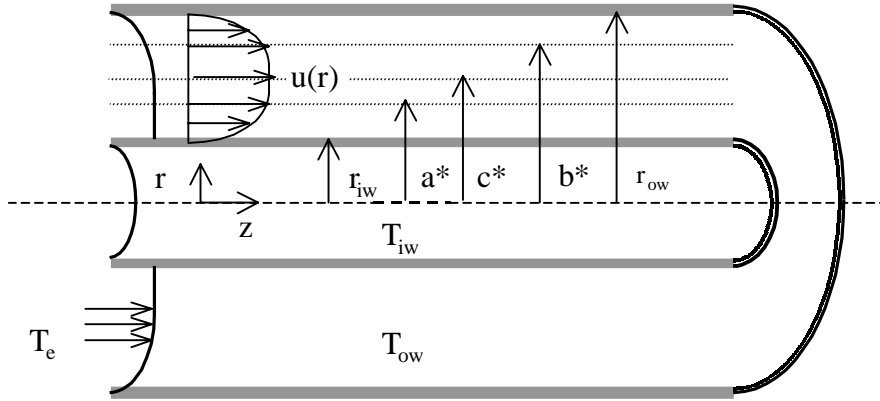


Figure 1 - Geometry and coordinate system of the problem

The velocity profile given by Eqs. (3) for a Bingham plastic fluid is split in three distinct regions, one  $a^* \leq r \leq b^*$  which denotes the plug-flow region where  $|\tau_{rz}| < \tau_0$ , and the fluid behaves like a solid plug, and other two regions for  $r_{iw} \leq r \leq a^*$  and for  $b^* \leq r \leq r_{ow}$  where  $|\tau_{rz}| \geq \tau_0$ , and refer to those parts of fluid which are in shear flow.

In the analysis of the thermal problem, we consider steady-state laminar forced convection heat transfer to hydrodynamically developed flow, in thermal entry region of incompressible non-newtonian fluid that follows the Bingham plastic model, described by Eqs. (1) and (3), inside concentric annular ducts maintained at prescribed wall temperatures  $T_{iw}$  and  $T_{ow}$  (Figure 1). The fluid enters the channel with a constant uniform temperature  $T_e$ . Axial heat conduction and viscous dissipation are neglected and the physical properties are considered temperature independent. Here, interest is given on the fundamental formulation where the boundary conditions are of first kind, either inner or outer wall duct in the following form:  $T_{iw} = T_e$  (case A) or  $T_{ow} = T_e$  (case B).

Then, the mathematical formulation of this heat transfer problem in dimensionless form is defined by:

$$W(R) \frac{\partial \theta(R, Z)}{\partial Z} = \frac{\partial}{\partial R} \left[ R \frac{\partial \theta(R, Z)}{\partial R} \right], \quad \text{in } \gamma < R < 1, \quad Z > 0 \quad (4.a)$$

subject to the inlet and boundary conditions:

$$\theta(R, 0) = 0, \quad \gamma \leq R \leq 1 \quad (4.b)$$

$$\theta(\gamma, Z) = 1 - m \quad \text{and} \quad \theta(1, Z) = m, \quad Z > 0 \quad (4.c, d)$$

where in the boundary conditions (4.c, d), the coefficient  $m$  identifies whether it refers to the case A ( $m = 1$ ) or to the case B ( $m = 0$ ).

In Eqs. (4) above the following dimensionless groups were used:

$$R = \frac{r}{r_{ow}}; \quad \gamma = \frac{r_{iw}}{r_{ow}}; \quad U(R) = \frac{u(r)}{u_m}; \quad W(R) = \frac{R U(R)}{4(1-\gamma)^2}; \quad Z = \frac{z}{D_h \text{Re} \text{Pr}} \quad (5.a-e)$$

$$\text{Re} = \frac{u_m D_h \rho}{\mu_0}; \quad \text{Pr} = \frac{\mu_0 c_p}{k}; \quad \theta(R, Z) = \begin{cases} \frac{T(r, z) - T_e}{T_{ow} - T_e}, & \text{for } m = 1 \\ \frac{T(r, z) - T_e}{T_{iw} - T_e}, & \text{for } m = 0 \end{cases} \quad (5.f-i)$$

where  $D_h = 2(r_{ow} - r_{iw})$  is the hydraulic diameter.

The velocity profile given by Eqs. (3) is written in dimensionless form by introducing the groups (5), or

$$U^-(R) = \frac{Y \gamma}{2(1-\gamma)} \left( 1 - \frac{R}{\gamma} \right) + \frac{f \text{Re} \gamma^2}{8(1-\gamma)^2} \left( 1 - \frac{R^2}{\gamma^2} \right) + \frac{f \text{Re} a b}{4(1-\gamma)^2} \ln \left( \frac{R}{\gamma} \right) \quad \text{for } \gamma \leq R \leq a \quad (6.a)$$

$$U^0(R) = \begin{cases} -\frac{Y(a-\gamma)}{2(1-\gamma)} - \frac{f \text{Re}(a^2 - \gamma^2)}{8(1-\gamma)^2} + \frac{f \text{Re} a b}{4(1-\gamma)^2} \ln \left( \frac{a}{\gamma} \right) \\ -\frac{Y(1-b)}{2(1-\gamma)} + \frac{f \text{Re}(1-b^2)}{8(1-\gamma)^2} + \frac{f \text{Re} a b}{4(1-\gamma)^2} \ln b \end{cases} \quad \text{for } a \leq R \leq b \quad (6.b, c)$$

$$U^+(R) = -\frac{Y(1-R)}{2(1-\gamma)} + \frac{f \text{Re}(1-R^2)}{8(1-\gamma)^2} + \frac{f \text{Re} a b}{4(1-\gamma)^2} \ln R \quad \text{for } b \leq R \leq 1 \quad (6.d)$$

and, the dimensionless bounds on the plug-flow region,  $a$  and  $b$ , and the dimensionless radial coordinate where the shear stress is zero,  $c$ , are related through the following equations:

$$a = b - \frac{2Y(1-\gamma)}{f \text{Re}}, \quad c = \sqrt{a b} \quad (7, 8)$$

The definitions of these quantities,  $a$ ,  $b$  and  $c$  are given below, as well as, of the additional groups employed in Eqs. (6)-(8) which are  $Y$  (the yield number) and  $f$  (the Fanning friction factor), i.e.,

$$a = \frac{a^*}{r_{ow}}; \quad b = \frac{b^*}{r_{ow}}; \quad c = \frac{c^*}{r_{ow}}; \quad Y = \frac{\tau_0 D_h}{\mu_0 u_m}; \quad f = \left( -\frac{dp}{dz} \right) \frac{D_h}{2 \rho u_m^2} \quad (9.a-e)$$

The Fanning friction factor and the dimensionless bounds on the plug-flow region are functions of the Reynolds and yield numbers. The determination of these quantities is obtained by satisfying the average flow velocity and by equalizing Eqs. (6.b) and (6.c), which together with Eq. (7) provide a system of three equations to find  $fRe$ ,  $a$  and  $b$ , once these quantities have been determined the parameter  $c$  is readily calculated from Eq. (8). Table 1 shows some results for these parameters described above, for different yield numbers,  $Y$ , and aspect ratios,  $\gamma$ . It can be observed that for increasing yield numbers the region of plug-flow increases as was expected. From this table the case  $Y = 0$  corresponds to the newtonian situation and in it, there is not a plug-flow region as verified by finding the same values for the parameters  $a$ ,  $b$  and  $c$ . It can also be noticed that for this situation of  $Y = 0$ , at high values of aspect ratios, for example  $\gamma = 0.9$ , the product  $fRe$  is near to that of the case of parallel-plates channel, i.e.,  $fRe \approx 24$ .

Table 1 - Product  $fRe$  and parameters  $a$ ,  $b$  and  $c$  computed from the present analysis

$\gamma$	$Y = 0$				$Y = 1$			
	$fRe$	$a$	$b$	$c$	$fRe$	$a$	$b$	$c$
0.1	22.343	0.4636	0.4636	0.4636	25.223	0.4232	0.4945	0.4574
0.3	23.461	0.6147	0.6147	0.6147	26.417	0.5861	0.6391	0.6120
0.5	23.812	0.7355	0.7355	0.7355	26.793	0.7160	0.7533	0.7344
0.7	23.949	0.8455	0.8455	0.8455	26.940	0.8341	0.8564	0.8452
0.9	23.996	0.9496	0.9496	0.9496	26.990	0.9458	0.9532	0.9495
$\gamma$	$Y = 5$				$Y = 10$			
0.1	36.459	0.3321	0.5790	0.4385	49.877	0.2797	0.6406	0.4233
0.3	37.941	0.5184	0.7029	0.6037	51.668	0.4766	0.7476	0.5969
0.5	38.413	0.6687	0.7989	0.7309	52.242	0.6386	0.8300	0.7280
0.7	38.597	0.8061	0.8838	0.8441	52.468	0.7880	0.9024	0.8432
0.9	38.660	0.9366	0.9624	0.9494	52.544	0.9304	0.9685	0.9493

Now, attention is focussed for the solution of the heat transfer problem given by Eqs. (4) through the classical integral transform technique (Mikhailov and Özisik, 1984; Cotta, 1993). In order to make the boundary conditions (4.c, d) homogeneous, so that a better computational performance in the series expansion can be obtained, a splitting-up procedure is proposed as (Mikhailov, 1977; Mikhailov and Özisik, 1984):

$$\theta(R, Z) = \theta_p(R) + \theta_h(R, Z) \quad (10)$$

After introducing Eq. (10) into Eqs. (4), the following problems for the potentials  $\theta_p(R)$  and  $\theta_h(R, Z)$  are obtained:

$$\frac{d}{dR} \left[ R \frac{d\theta_p(R)}{dR} \right] = 0, \quad \text{in } \gamma < R < 1 \quad (11.a)$$

$$\theta_p(\gamma) = 1 - m, \quad \theta_p(1) = m \quad (11.b,c)$$

with its respective solution:

$$\theta_p(R) = m + (1 - 2m) \frac{\ln R}{\ln \gamma} \quad (12)$$

and,

$$W(R) \frac{\partial \theta_h(R, Z)}{\partial Z} = \frac{\partial}{\partial R} \left[ R \frac{\partial \theta_h(R, Z)}{\partial R} \right], \quad \text{in } \gamma < R < 1, Z > 0 \quad (13.a)$$

with inlet and boundary conditions:

$$\theta_h(R, 0) = -\theta_p(R), \quad \gamma \leq R \leq 1 \quad (13.b)$$

$$\theta_h(\gamma, Z) = \theta_h(1, Z) = 0, \quad Z > 0 \quad (13.c,d)$$

The homogeneous problem defined above by Eqs. (13) can also be solved by the classical integral transform technique. Then, following the procedures in the application of this technique, the appropriate auxiliary eigenvalue problem is taken as:

$$\frac{d}{dR} \left[ R \frac{d\psi_i(R)}{dR} \right] + \mu_i^2 W(R) \psi_i(R) = 0, \quad \text{in } \gamma < R < 1 \quad (14.a)$$

$$\psi_i(\gamma) = 0; \quad \psi_i(1) = 0 \quad (14.b,c)$$

where  $\psi_i(R)$  and  $\mu_i$  are, respectively, the eigenfunctions and eigenvalues. The eigenvalue problem allows for the development of the following integral transform pair:

$$\theta_h(R, Z) = \sum_{i=1}^{\infty} \frac{1}{N_i} \psi_i(R) \bar{\theta}_{h,i}(Z), \quad \text{inversion} \quad (15.a)$$

$$\bar{\theta}_{h,i}(Z) = \int_{\gamma}^1 W(R) \psi_i(R) \theta_h(R, Z) dR, \quad \text{transform} \quad (15.b)$$

and the norm  $N_i$  is calculated from

$$N_i = \int_{\gamma}^1 W(R) \psi_i^2(R) dR \quad (16)$$

Now, Eq. (13) is integral transformed by operating it with  $\int_{\gamma}^1 \psi_i(R) dR$ , to yield the following ordinary differential equation for the transformed potential,  $\bar{\theta}_{h,i}(Z)$ :

$$\frac{d\bar{\theta}_{h,i}(Z)}{dZ} + \mu_i^2 \bar{\theta}_{h,i}(Z) = 0 \quad (17.a)$$

with the transformed potential inlet condition given by:

$$\bar{\theta}_{h,i}(0) = \bar{f}_i = - \int_{\gamma}^1 W(R) \psi_i(R) \theta_p(R) dR \quad (17.b)$$

The solution for the transformed potential  $\bar{\theta}_{h,i}(Z)$  is readily obtained as:

$$\bar{\theta}_{h,i}(Z) = \bar{f}_i \exp(-\mu_i^2 Z) \quad (18)$$

Then, introducing Eq.(18) into the inversion formula (15.a), the solution for  $\theta_h(R, Z)$  is determined in the form:

$$\theta_h(R, Z) = \sum_{i=1}^{\infty} \frac{\bar{f}_i}{N_i} \psi_i(R) \exp(-\mu_i^2 Z) \quad (19)$$

Thus, by combining Eq. (12) for  $\theta_p(R)$  with Eq. (19) for  $\theta_h(R, Z)$ , the complete solution for the original potential  $\theta(R, Z)$  is written as:

$$\theta(R, Z) = m + (1 - 2m) \frac{\ln R}{\ln \gamma} + \sum_{i=1}^{\infty} \frac{\bar{f}_i}{N_i} \psi_i(R) \exp(-\mu_i^2 Z) \quad (20)$$

From Eq. (20) for  $\theta(R, Z)$  quantities of practical interest such as average flow temperature and Nusselt numbers can be determined.

The average flow temperature  $\theta_{av}(Z)$  is defined as:

$$\theta_{av}(Z) = \int_{\gamma}^1 W(R) \theta(R, Z) dR \Big/ \int_{\gamma}^1 W(R) dR \quad (21)$$

Thus, by introducing Eq. (20) into Eq. (21), the  $\theta_{av}(Z)$  is readily obtained from the following equation:

$$\theta_{av}(Z) = m + \frac{8(1-\gamma)}{(1+\gamma)} \frac{(1-2m)}{\ln \gamma} \left( \int_{\gamma}^1 W(R) \ln R dR \right) + \frac{8(1-\gamma)}{(1+\gamma)} \sum_{i=1}^{\infty} \frac{\bar{f}_i}{N_i} \bar{h}_i \exp(-\mu_i^2 Z) \quad (22)$$

where,

$$\bar{h}_i = \int_{\gamma}^1 W(R) \psi_i(R) dR \quad (23)$$

The local Nusselt numbers at inner and outer walls are given by:

$$Nu_{iw}(Z) = -2(1-\gamma) \frac{\left. \frac{\partial \theta(R, Z)}{\partial R} \right|_{R=\gamma}}{(1-m) - \theta_{av}(Z)}, \quad Nu_{ow}(Z) = 2(1-\gamma) \frac{\left. \frac{\partial \theta(R, Z)}{\partial R} \right|_{R=1}}{m - \theta_{av}(Z)} \quad (24, 25)$$

By taking the derivative of Eq. (20) and evaluating it at  $R = \gamma$  or  $R = 1$ , in conjunction with Eq. (22) for the average flow temperature  $\theta_{av}(Z)$ , the solutions for the local Nusselt numbers at inner and outer walls can be readily determined from Eqs. (24) and (25), respectively.

### 3. RESULTS AND DISCUSSION

First, the eigenquantities related to eigenvalue problem (14) were obtained by two approaches, generalized integral transform technique (Cotta, 1993) and sign-count method (Mikhailov and Özisik, 1984). The results obtained through the two approaches are in perfect agreement, but due to space limitations they are not listed here. Then the average temperature,  $\theta_{av}(Z)$ , and local Nusselt numbers,  $Nu_{iw}(Z)$  and  $Nu_{ow}(Z)$ , for the two cases of fundamental situations of the boundary conditions were calculated.

In Table 2, the present results are validated against previous results for Newtonian fluids (i.e.,  $Y = 0$ ) presented by Shah and London (1978), in thermal entry region, for the following values of aspect ratio  $\gamma = 0.1$ ; 0.25 and 0.5. From these table, it can be noticed that the results are in excellent agreement, providing a direct validation of the numerical code developed in this work.

Table 2 - Local Nusselt numbers and average flow temperature in thermal entry region for different values of aspect ratio and  $Y = 0$  (Newtonian fluids)

$\gamma$	$Z$	Case A			Case B		
		$Nu_{iw}$	$Nu_{ow}$	$\theta_{av}$	$Nu_{iw}$	$Nu_{ow}$	$\theta_{av}$
<b>0.10</b>	1.0E-5	—	52.340* 52.336+	0.00282* 0.00287+	80.328* 80.324+	—	0.00047* 0.00043+
	1.0E-4	—	23.890 23.888	0.01303 0.01308	40.770 40.767	—	0.00215 0.00210
	1.0E-3	—	10.913 10.912	0.05827 0.05832	22.257 22.192	—	0.01099 0.01094
	1.0E-2	0.1661* 0.1550+	5.3590 5.3590	0.24529 0.24530	13.761 13.762	0.0664* 0.0640+	0.06134 0.06131
	1.0E-1	9.7921 9.7920	3.4131 3.4130	0.70058 0.70058	10.702 10.702	2.9332 2.9330	0.23388 0.23388
	$\infty$	10.459 10.459	3.0953 3.0950	0.74744 0.74744	10.459 10.459	3.0953 3.0950	0.25256 0.25256
<b><math>\gamma</math></b>	<b><math>Z</math></b>	<b><math>Nu_{iw}</math></b>	<b><math>Nu_{ow}</math></b>	<b><math>\theta_{av}</math></b>	<b><math>Nu_{iw}</math></b>	<b><math>Nu_{ow}</math></b>	<b><math>\theta_{av}</math></b>
<b>0.25</b>	1.0E-5	—	53.417* 53.414+	0.00254* 0.00257+	66.558* 66.555+	—	0.00082* 0.00079+
	1.0E-4	—	24.439 24.438	0.01173 0.01176	32.069 32.067	—	0.00378 0.00375
	1.0E-3	—	11.204 11.204	0.05270 0.05273	16.139 16.138	—	0.01829 0.01826
	1.0E-2	0.1335* 0.1300+	5.5175 5.5170	0.22474 0.22473	9.0751 9.0730	0.0813* 0.0830+	0.09229 0.09229
	1.0E-1	6.1408 6.1410	3.4936 3.4940	0.63474 0.63474	6.6405 6.6410	3.1201 3.1200	0.31232 0.31231
	$\infty$	6.4714 6.4710	3.2670 3.2670	0.66880 0.66880	6.4714 6.4710	3.2670 3.2670	0.33120 0.33120
<b><math>\gamma</math></b>	<b><math>Z</math></b>	<b><math>Nu_{iw}</math></b>	<b><math>Nu_{ow}</math></b>	<b><math>\theta_{av}</math></b>	<b><math>Nu_{iw}</math></b>	<b><math>Nu_{ow}</math></b>	<b><math>\theta_{av}</math></b>
<b>0.50</b>	1.0E-5	—	54.736* 54.733+	0.00218* 0.00220+	60.544* 60.543+	—	0.00122* 0.00121+
	1.0E-4	—	25.144 25.142	0.01005 0.01007	28.456 28.455	—	0.00565 0.00563
	1.0E-3	—	11.606 11.605	0.04548 0.04549	13.702 13.701	—	0.02644 0.02642
	1.0E-2	0.1177* 0.1160+	5.7614 5.7610	0.19783 0.19773	7.2460 7.2760	0.0932* 0.0920+	0.12498 0.12488
	1.0E-1	4.6715 4.6710	3.6979 3.6980	0.56327 0.56325	5.0370 5.0370	3.3737 3.3740	0.38997 0.38995
	$\infty$	4.8890 4.8890	3.5204 3.5200	0.59019 0.59018	4.8890 4.8890	3.5204 3.5200	0.40981 0.40982

\* Present work, + Shah and London (1978)

In Figs. 2 - 7 the results of axial distribution of the local Nusselt numbers along the thermal entry region are presented, for different yield numbers and aspect ratios. It is verified an increasing of the Nusselt numbers for increasing yield numbers; this fact can be explained by high gradients in the velocity field near to the wall when the yield number increases. This effect tends to disappear for the fully-developed regions where the curves are practically coincident.



Finally, from these figures it can be also observed that the Nusselt numbers for the two cases studied here,  $Nu_{iw}(Z)$  and  $Nu_{ow}(Z)$ , tend to the same distribution when the aspect ratio increases. For example, for the case of aspect ratio  $\gamma = 0.9$ , which practically represents a parallel-plates channel, this symmetry is clearly observed.

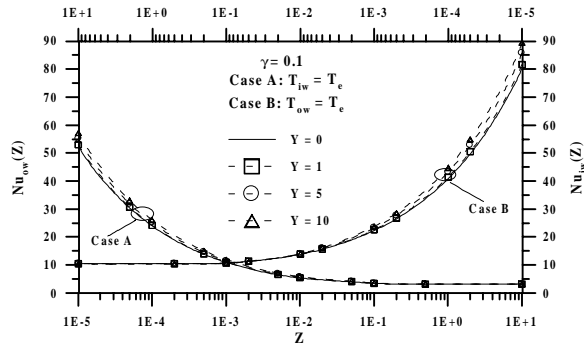


Figure 2 - Local Nusselt numbers in thermal entry region for different values of yield numbers and  $\gamma = 0.1$

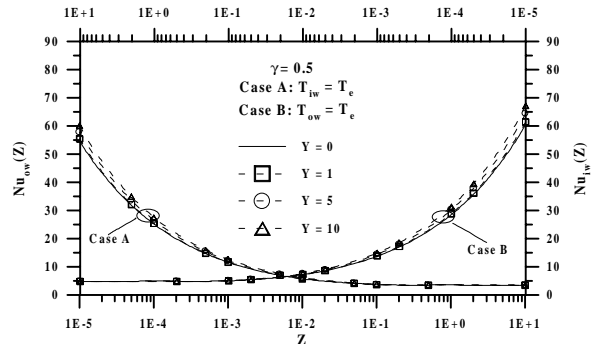


Figure 5 - Local Nusselt numbers in thermal entry region for different values of yield numbers and  $\gamma = 0.5$

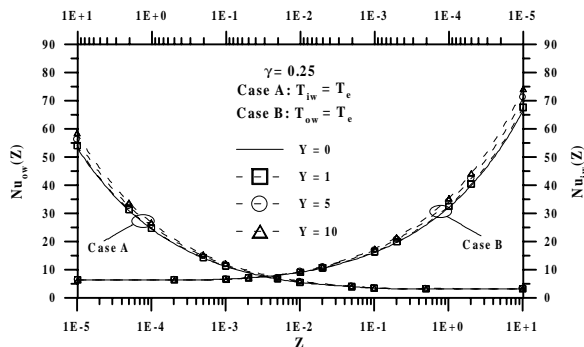


Figure 3 - Local Nusselt numbers in thermal entry region for different values of yield numbers and  $\gamma = 0.25$

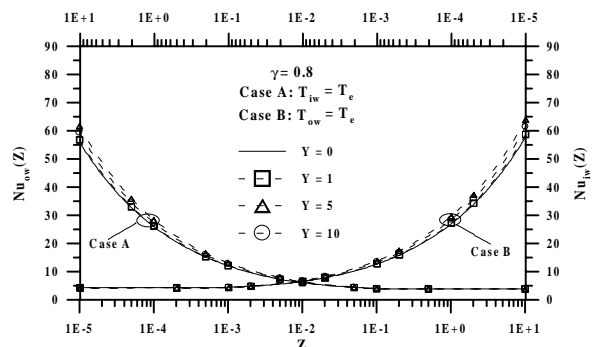


Figure 6 - Local Nusselt numbers in thermal entry region for different values of yield numbers and  $\gamma = 0.8$

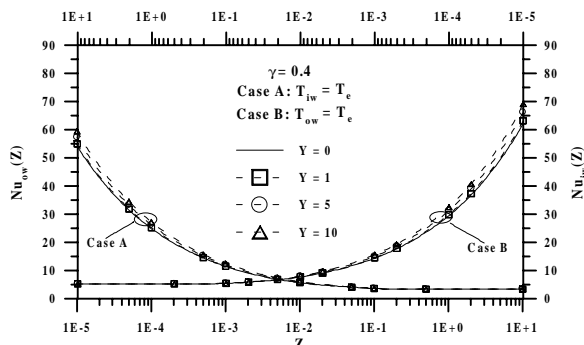


Figure 4 - Local Nusselt numbers in thermal entry region for different values of yield numbers and  $\gamma = 0.4$

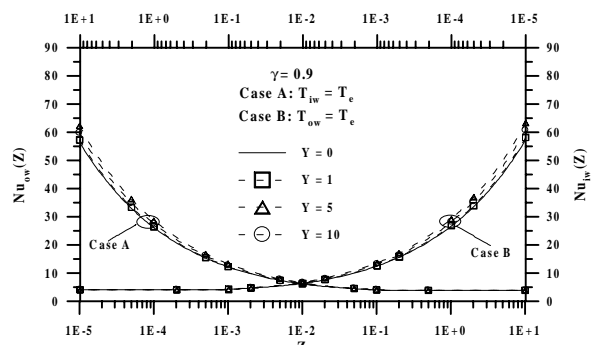


Figure 7 - Local Nusselt numbers in thermal entry region for different values of yield numbers and  $\gamma = 0.9$

#### 4. CONCLUSIONS

The problem of laminar convective heat transfer in thermal entry and fully-developed flow regions of Bingham plastics, for two fundamental situations of boundary conditions of first kind in concentric annular ducts, has been analyzed by the classical integral transform

technique in conjunction with the sign-count method and generalized integral transform technique for the solution of the related eigenvalue problem.

Results for axial distributions of  $\theta_{av}$ ,  $Nu_{iw}(Z)$  (case A) and  $Nu_{ow}(Z)$  (case B) were presented in tabular form which were validated with previous results for newtonian fluids. Results of Nusselt numbers were graphically presented for different values of aspect ratios and yield numbers in thermal entry and fully-developed regions.

## REFERENCES

- Anshus, B. E., 1974, Bingham Plastic Flow in Annuli, *Ind. Eng. Chem., Fundam.*, vol. 13, pp. 162-164.
- Bird, R. B., Armstrong, R. C. & Hassager, O., 1987, *Dynamics of Polymeric Liquids*, vol. 1, John Wiley, 2<sup>nd</sup> Ed., New York.
- Bird, R. B., Dai, G. C. & Yarusso, B. J., 1982, The Rheology and Flow of Viscoplastic Materials, *Reviews in Chemical Engineering*, vol. 1, pp. 1-70.
- Blackwell, B. F., 1985, Numerical Solution of the Graetz Problem for a Bingham Plastic in Laminar Tube Flow with Constant Wall Temperature, *Journal of Heat Transfer*, vol. 107, pp. 466-468.
- Cotta, R. M., 1993, *Integral Transforms in Computational Heat and Fluid Flow*, CRC Press, Boca Raton.
- Forrest, G. & Wilkinson, W. L., 1973, Laminar Heat Transfer to Temperature-Dependent Bingham Fluids in Tubes, *Int. J. Heat Mass Transfer*, vol. 16, pp. 2377-2391.
- Fredrickson, A. G. & Bird R. B., 1958, Non-Newtonian Flow in Annuli, *Industrial and Engineering Chemistry*, vol. 50, pp. 347-352.
- Laird, W. M., 1957, Slurry and Suspension Transport, *Industrial and Engineering Chemistry*, vol. 49, pp. 138-141.
- Mendes, P. R. S. & Naccache, M. F., 1995, Heat Transfer to Herschel-Bulkley Fluids in Laminar Fully Developed Flow through Tubes, *Proc. of the 13<sup>th</sup> Brazilian Congress of Mechanical Engineering, XIII COBEM*, December, Belo Horizonte, Brazil.
- Min, T., Choi, H. G., Yoo, J. Y. & Choi, H., 1997, Laminar Convective Heat Transfer of a Bingham Plastic in a Circular Pipe-II. Numerical Approach-Hydrodynamically Developing Flow and Simultaneously Developing Flow, *Int. J. Heat Mass Transfer*, vol. 40, pp. 3689-3701.
- Mikhailov, M. D. & Özisik, M. N., 1984, *Unified Analysis and Solutions of Heat and Mass Diffusion*, John Wiley, New York.
- Mikhailov, M. D., 1977, Splitting Up of Heat-Conduction Problems, *Letters Heat Mass Transf.*, vol. 4, pp. 163-166.
- Nouar, C., Devienne, R. & Lebouché, M., 1994, Convection Thermique pour un Fluide de Herschel-Bulkley dans la Région d'Entrée d'une Conduite, *Int. J. Heat Mass Transfer*, vol. 37, pp. 1-12.
- Nouar, C., Lebouché, M., Devienne, R. & Riou, C., 1995, Numerical Analysis of the Thermal Convection for Herschel-Bukley Fluids, *Int. J. Heat and Fluid Flow*, vol. 16, pp. 223-231.
- Shah, R. K. & London, A. L., 1978, *Laminar Flow Forced Convection in Ducts*, Supplement 1 to *Advances in Heat Transfer*, eds. T. F. Irvine and J. P. Hartnett, Academic Press, New York.
- Vradis, G. C. & Hammad, K. J., 1995, Heat Transfer in Flows of Non-Newtonian Bingham Fluids through Axisymmetric Sudden Expansions and Contractions, *Numerical Heat Transfer, Part A*, vol. 28, pp. 339-353.
- Vradis, G. C., Dougher, J. & Kumar, S., 1993, Entrance Pipe Flow and Heat Transfer for a Bingham Plastic, *Int. J. Heat Mass Transfer*, vol. 36, pp. 543-552.